Appl Phys B
DOI 10.1007/s00340-009-3682-x

**Applied Physics B**
**Lasers and Optics**

# EOM sideband phase characteristics for the spaceborne gravitational wave detector LISA

**S. Barke · M. Tröbs · B. Sheard · G. Heinzel · K. Danzmann**

Received: 2 June 2009 / Revised version: 6 July 2009


**Abstract** The Laser Interferometer Space Antenna (LISA) is a joint ESA/NASA mission proposed to observe gravitational waves. One important noise source in the LISA phase measurement will be on-board reference oscillators. An inter-spacecraft clock tone transfer chain will be necessary to remove this non-negligible phase noise in post processing. One of the primary components of this chain are electro-optic modulators (EOMs). At modulation frequencies of 2 GHz, we characterise the excess phase noise of a fibre-coupled integrated EOM in the LISA measurement band (0.1 mHz to 1 Hz). The upper phase noise limit was found to be almost an order of magnitude better than required by the LISA mission. In addition, the EOM's phase dependence on temperature and optical power was determined. The measured coefficients are within a few milliradians per kelvin and per watt respectively and thereby negligible with the expected on-board temperature and laser power stability.

**PACS** 04.80.Nn · 78.20.Jq · 42.60.Mi

## 1 Introduction

The Laser Interferometer Space Antenna (LISA) [1], a joint ESA/NASA mission, will observe gravitational waves emitted by binary star systems at frequencies from 0.1 mHz to 1 Hz. The three LISA spacecraft, which are separated by 5 million kilometers, will form a laser interferometer designed to have its highest sensitivity at 3 mHz. At this frequency, gravitational waves with a strain down to $7 \times 10^{-21}\,(1/\sqrt{\text{Hz}})$ will be observable. At a separation distance of 5 million kilometers, these gravitational waves correspond to a change in observed spacecraft separation of

$$\Delta l_{\text{S/C}} \approx \frac{7 \times 10^{-21}}{2} \frac{1}{\sqrt{\text{Hz}}} \times 5 \times 10^{9}\,\text{m} < 20\,\frac{\text{pm}}{\sqrt{\text{Hz}}}. \tag{1}$$

As shown in Fig. 1, top right, the incoming laser light from the remote spacecraft (S/C 1) is collected by a telescope and heterodyned at the receiving spacecraft with a local laser beam. Due to laser frequency offsets and Doppler shifts from spacecraft motion, the frequency difference between both beams varies by up to $f_{\text{het}} = 20$ MHz during the one-year period. To determine the phase of the resulting beat note (and thereby path-length fluctuations due to gravitational waves), the RF output signal of the photodiode is compared to a reference frequency provided by an ultra-stable oscillator (USO).

Errors in the sampling time, $\Delta t$, of the analogue-to-digital converter (ADC), triggered by the USO, produce a phase error indistinguishable from a change in separation. Since the additional instrumental phase noise detected by the phasemeter must be small compared to the design sensitivity, a noise level equivalent to a spacecraft displacement of $1\,\text{pm}/\sqrt{\text{Hz}}$ is commonly allocated to the phase measurement system. This translates to a phase noise requirement of

$$\Delta\phi_{1\text{ pm}} < \frac{1\,\text{cycle}}{1064\,\text{nm}} \times \frac{1\,\text{pm}}{\sqrt{\text{Hz}}} \approx 1\,\frac{\mu\text{cycles}}{\sqrt{\text{Hz}}} \approx 6\,\frac{\mu\text{rad}}{\sqrt{\text{Hz}}}. \tag{2}$$

The resulting USO timing fidelity requirement is beyond the performance of any feasible reference oscillator available for LISA [2, 3]. Therefore, the phase noise of the USO used is not negligible and needs to be removed.

S. Barke (✉) · M. Tröbs · B. Sheard · G. Heinzel · K. Danzmann
Albet Einstein Institute Hannover, Max Planck Institute
for Gravitational Physics and Leibniz University Hannover,
Callinstr. 38, 30167 Hannover, Germany
e-mail: simon.barke@aei.mpg.de

Published online: 18 August 2009

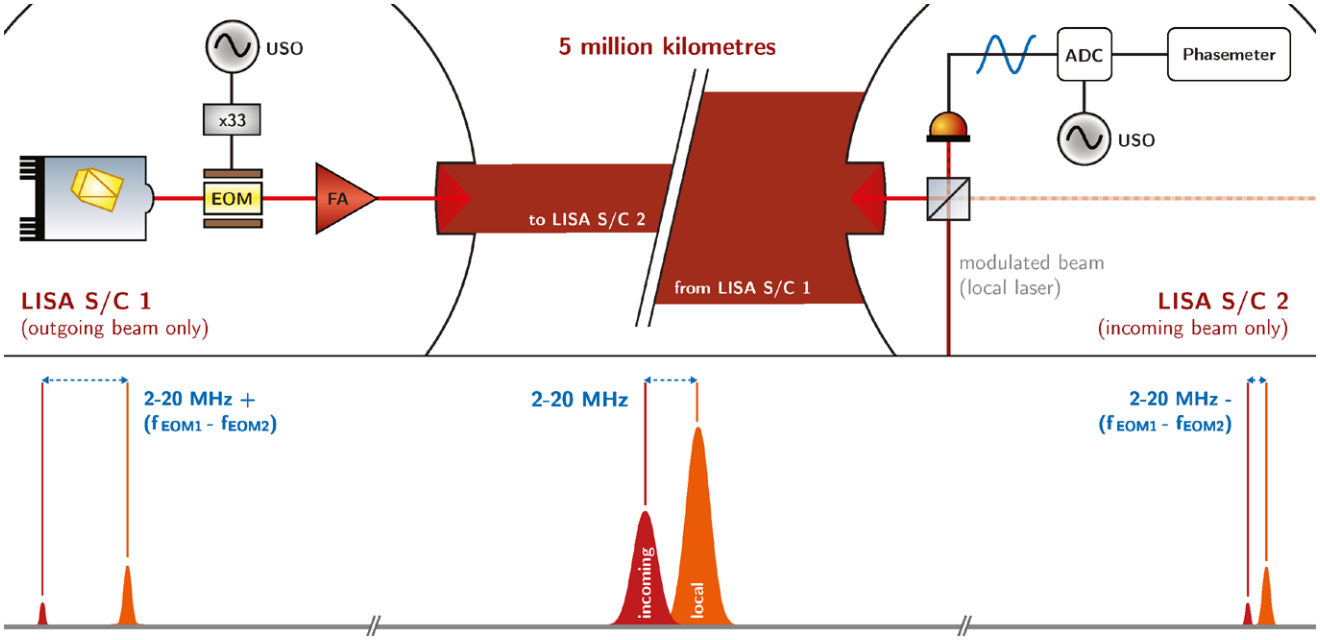


**Fig. 1** LISA inter-spacecraft clock tone transfer scheme: LISA satellite, outgoing beam only (*top left*), LISA satellite, incoming beam only (*top right*), resulting frequency spectrum (*bottom*)

## 2 Inter-spacecraft clock tone transfer chain

The basic idea to remove the phase noise of the USOs is to measure it and send this information to Earth where the phase noise can be cancelled from the measurement data in post processing. Measuring the USO phase noise locally is impossible in the current baseline design. Therefore, an inter-spacecraft clock tone transfer scheme was proposed.

### 2.1 Practical implementation

For the clock tone transfer, a frequency multiplier (Fig. 1, left) is used to scale the USO frequency $f_{\mathrm{USO}} \approx 60$ MHz to a modulation frequency $f_{\mathrm{mod}} \approx 2$ GHz [4]. The upconverted signal is then modulated onto the laser beam by an electro-optic modulator (EOM) [5], while the local phasemeter's ADC is triggered directly by the USO.

Since we are not aware of compact and robust EOMs with low half-wave voltage that are able to handle optical powers larger than 300 mW, modulation takes place at a low power level. The modulated laser light is then amplified by a fibre amplifier to obtain the required power of at least 1 W. The main carrier signal is transmitted, together with the modulation sidebands, to the receiving spacecraft. As shown in Fig. 1 (right), the incoming light is heterodyned with a local laser beam which is modulated by the same principle at a slightly different frequency.

A photodetector now detects three beat notes: the carrier–carrier beat at a frequency up to 20 MHz and two sideband–sideband beats (Fig. 1, bottom). Since the sidebands were imposed onto the laser beams by a signal phase locked to the USO signal, the sideband–sideband beat notes (at least one of them also below 20 MHz) contain information about the USO phase noise. Using this information, the USO noise can in principle be removed to acceptable levels [6]. Due to the sideband–sideband beat measurement, there is no need for ultra-high-frequency (UHF) electronics at the receiving end.

### 2.2 Requirement on transfer chain components

The components of the clock tone transfer chain might add excess phase noise to the sidebands, which is referred to as ancillary modulation error (AME). Unfortunately, there is no easy way to measure the excess noise on board the transmitting spacecraft at a point after the fibre amplifier. Hence, for the clock transfer and USO noise cancellation scheme to work properly, the phase between the optical USO signal (the optical clock tone imprinted by the EOM) and the electrical USO signal must not exceed the allowed phase noise equivalent to a spacecraft displacement of $1\,\mathrm{pm}/\sqrt{\mathrm{Hz}}$ (2).

Taking into account that the magnitude of a phase shift in a signal being upconverted by a frequency multiplier is increased linearly by the multiplication factor $(f_{\mathrm{mod}}/f_{\mathrm{USO}})$ [7], we therefore can derive a relaxed AME requirement of

$$\Delta\phi_{\mathrm{AME}} < \Delta\phi_{1\mathrm{pm}} \times \frac{f_{\mathrm{USO}}}{f_{\mathrm{het}}} \times \frac{f_{\mathrm{mod}}}{f_{\mathrm{USO}}} \approx 6 \times \frac{2\ \mathrm{GHz}}{20\ \mathrm{MHz}}\ \frac{\mu\mathrm{rad}}{\sqrt{\mathrm{Hz}}}. \tag{3}$$

With respect to the designed LISA sensitivity, we can state a frequency-dependent AME requirement given by

$$\Delta\phi_{\mathrm{AME}}(f) < 0.6 \times \sqrt{1 + \left(\frac{2.8 \times 10^{-3}\,\mathrm{Hz}}{f}\right)^4}\ \frac{\mathrm{mrad}}{\sqrt{\mathrm{Hz}}}, \quad (4)$$

which increases as $1/f^2$ for frequencies below 2.8 mHz.

### 2.3 Phase characteristics of transfer chain components

Experiments are essential to characterise suitable components and to find devices with sufficient phase stability to be used for the clock tone transfer chain. Multipliers have not been studied so far. Efforts on characterising fibre amplifiers, optical fibre cables and UHF cable assemblies are in progress at the Albert Einstein Institute in Hannover. Fibre amplifiers meeting the phase stability requirements recently have been found [8].

This paper presents measurements of the AME induced during the modulation process by the EOM itself. EOM phase characteristics were investigated previously for pairs of EOMs (differential processing of sideband pairs) at modulation frequencies up to 8 GHz [9]. The advantages of such high modulation frequencies are: (i) less sideband power is needed in order for clock calibration noise to be 1/10 of the carrier–carrier shot-noise limit and (ii) the relaxation upon the phase stability requirements is higher. The disadvantages, however, are a higher electrical power necessary for generating sidebands at higher frequencies and all common problems involved with UHF electronics. Hence, a lower sideband frequency as proposed in [10] is desirable. Since the two EOMs involved in one LISA sideband–sideband beat note are exposed to different environmental disturbances, we investigated the phase characteristics of a single EOM sideband as one isolated noise contribution.

## 3 LISA EOM candidate being tested

The EOM used for the practical LISA case must offer broadband phase modulation. The only modulators known to the authors allowing a phase modulation for frequencies from 100 Hz to as high as 10 GHz for selected models are fibre-coupled integrated EOMs. In addition, these EOMs are preferable for LISA due to their low half-wave voltage.

### 3.1 Jenoptik EOM specifications

Figure 2 shows the fibre-coupled integrated optical phase modulator by Jenoptik which we used for our research on the sideband phase stability. This EOM is polarisation maintaining and allows broadband phase modulation for frequencies up to 3 GHz.

**Fig. 2** Fibre-coupled integrated optical phase modulator by Jenoptik (*bottom right*: waveguide substrate)

The electro-optic medium used is a waveguide made of magnesium oxide doped lithium niobate (MgO:$LiNbO_3$) which provides a high damage threshold. Single-mode fibres are used to couple the light in and out of the EOM with a typical overall insertion loss of 4 dB. The maximum optical input power was limited to 300 mW; the maximum voltage was given by 40 $V_{pp}$.

By connecting the EOM output to a fibre-coupled confocal scanning Fabry–Perot interferometer, we determined the modulation efficiency at a modulation frequency ($f_{\mathrm{mod}}$) of ∼2 GHz to be 0.37 rad/V, which is equivalent to a half-wave voltage of 8.6 V.

### 3.2 Potential phase noise sources

There are several effects in the ferroelectric substrate of the optical waveguides used in integrated EOMs which can add excess phase noise to the sidebands. A heat-induced expansion will change the length of the waveguide and thereby the optical path length, which leads to an unwanted phase shift. The waveguide's refractive index is not constant over temperature, which is also referred to as the thermo-optic effect. Due to the material's pyroelectricity, changes in temperature can produce an electric potential (pyroelectric effect). This potential will then shift the phase of the light due to the linear electro-optic effect (Pockels effect) of lithium niobate [11]. Furthermore, for lithium niobate the refractive index decreases in response to higher optical powers, which is referred to as the photorefractive effect [12].

The thermal expansion, the thermo-optic effect and the pyroelectric effect do not only affect the EOM itself but—in the case of fibre-coupled EOMs—also the output fibre where the sideband's phase is shifted in relation to the carrier. The total magnitude of the phase noise added by the EOM to generated sidebands is difficult to predict and may even depend on the individual waveguide quality. Thus, we characterised the magnitude of these effects empirically.

## 4 Measuring EOM phase characteristics

### 4.1 EOM sideband phase noise measurement setup

Figure 3 shows a schematic of the setup used to measure the phase noise of a single EOM sideband. Two lasers at 1064 nm (L1 and L2) were offset phase locked to $f_{\mathrm{ref}} = 2\,\mathrm{GHz} + 1.6\,\mathrm{kHz}$ with one beam (L1) sent through the EOM under test driven by a signal at $f_{\mathrm{mod}} = 2$ GHz. Both laser beams were heterodyned at a beam splitter and sent to a photodiode where different heterodyne frequencies were detected: the two carriers beating against each other and the two sidebands of laser L1 beating against the carrier of laser L2.

In a simplified description omitting the spatial mode and polarisation of the electrical fields, the two detectable beatnote signal amplitudes within the photodetector bandwidth are: (i) for the carrier–carrier signal at 2 GHz + 1.6 kHz,

$$U_{\mathrm{HF}} \propto A_{\mathrm{L1}} J_0(m) A_{\mathrm{L2}} \times \cos(2\pi f_{\mathrm{ref}} t), \tag{5}$$

and (ii) for the sideband–carrier signal at 1.6 kHz,

$$U_{\mathrm{LF}} \propto A_{\mathrm{L1}} J_1(m) A_{\mathrm{L2}} \times \cos\left[2\pi (f_{\mathrm{ref}} - f_{\mathrm{mod}})t - \phi_{\mathrm{EOM}-}(t)\right], \tag{6}$$

where $\phi_{\mathrm{EOM}-}(t)$ is the phase noise of the lower sideband as shown in Fig. 4. $A_{\mathrm{L1}}$ and $A_{\mathrm{L2}}$ are the electrical field amplitudes of the two laser beams (L1 and L2), $m$ is the modulation index which is proportional to the amplitude of the signal driving the EOM ($m \propto A_{\mathrm{mod}}$) and $J_n(m)$ is the Bessel function of the first kind, order $n$, evaluated at $m$. Since we used a low modulation index of $m = 0.65$—or 12% of the carrier power in a single sideband—we ignore the higher-order sidebands [13].

The carrier–carrier beat note (5) was passed to an electronic mixer and mixed down with the same signal driving the EOM. Considering only the low-pass-filtered signal of the mixer output, we thereby obtained another signal at 1.6 kHz:

$$U_{\mathrm{Mix}} \propto \frac{A_{\mathrm{L1}} J_0(m) A_{\mathrm{L2}} A_{\mathrm{mod}}}{2} \times \cos\left[2\pi (f_{\mathrm{ref}} - f_{\mathrm{mod}})t\right]. \tag{7}$$

A DC voltage proportional to the amplitude of the $U_{\mathrm{Mix}}$ signal was passed to a loop filter which was connected to both laser diode current drivers, thus stabilising the beatnote power. This technique suppressed unwanted phase shifts due to power fluctuations within the UHF electronics.

The EOM phase noise measurement required the phase information of the two signals described by (6) and (7). A software phasemeter operating with the same principle as the LISA Technology Package (LTP) phasemeter was used for this purpose [14]. After determining the phase of both signals (where $\phi_{\mathrm{mix}}$ and $\phi_{\mathrm{LF}}$ are the phases of $U_{\mathrm{mix}}$ and $U_{\mathrm{LF}}$, respectively), we computed the differential phase

$$\Delta\phi = \phi_{\mathrm{mix}} - \phi_{\mathrm{LF}}. \tag{8}$$

The spectral phase noise densities of the differential phases were then calculated by the LPSD program [15, 16]. One finds that the phase noise of the lower EOM sideband ($\phi_{\mathrm{EOM}-}(t)$) is observable in the differential phase $\Delta\phi$. Further phase noise induced by the frequency generators and

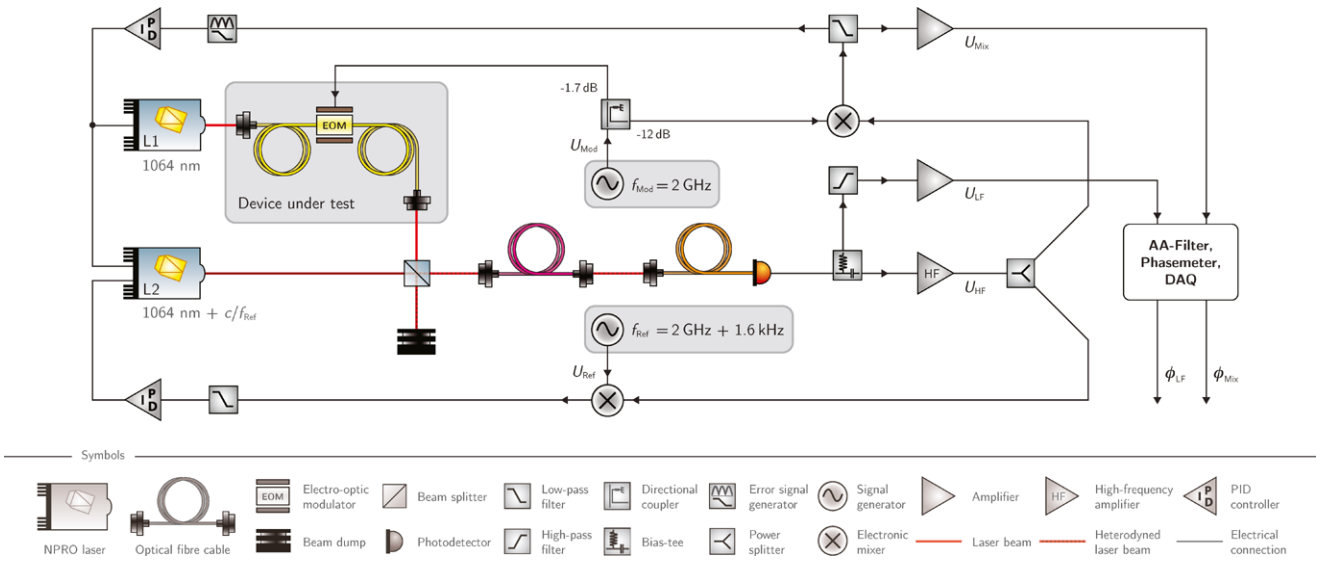


**Fig. 3** Setup for measuring the phase characteristics of a single EOM sideband at 2 GHz (schematic): two lasers (one modulated by an EOM at $f_{\mathrm{Mod}} = 2\,\mathrm{GHz}$) offset phase locked to $f_{\mathrm{Ref}} = 2\,\mathrm{GHz} + 1.6\,\mathrm{kHz}$ were heterodyned and power stabilised with respect to the amplitude of the 2-GHz beat note by a second control loop

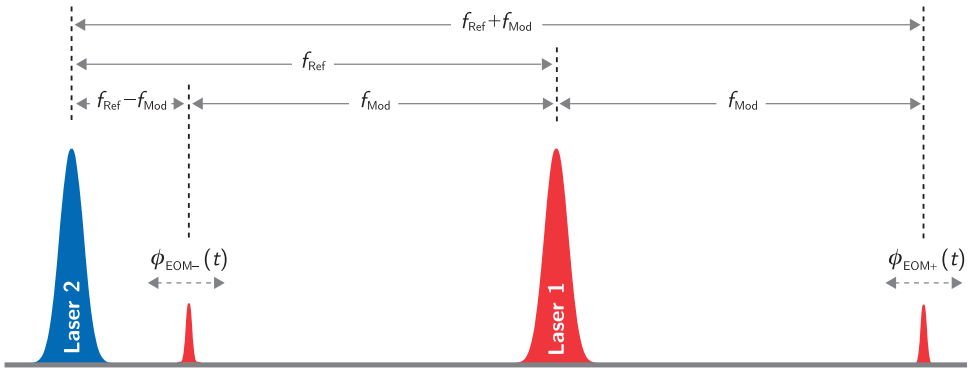


**Fig. 4** Frequency spectrum of measurement signals

the phase-locked loop (PLL) electronics is common mode and thereby cancel in the differential phase. However, noise induced by cables, photodiodes, UHF electronics and the EOM itself is not common mode and therefore visible in the differential phase $\Delta\phi$. Hence, the spectral phase noise density, calculated from a time series of $\Delta\phi$, represents an upper limit for the sideband phase noise induced by the EOM under test. Note that phase shifts common to carrier and both sidebands look like a frequency fluctuation of the laser and will be removed by the PLL.

Many setup components induced a phase shift of the 2-GHz signal due to a change in temperature. The phase–temperature relationship at a temperature of ∼22°C was measured to be ∼4 mrad/K m for electrical cables ('original minibend' by Astrolab, USA) and ∼0.6 mrad/K m for optical fibre cables (single-mode fibre cable by Schäfter + Kirchhoff). Environmental temperature fluctuations in our laboratory would have induced a phase noise higher than allowed by the LISA specification. For this reason all UHF electronics, the lasers, the optics and the EOM were isolated by extruded polystyrene boxes that provided a low thermal conductivity of 0.03 W/m K, and led to a temperature stability of about 0.1 K/Hz at $10^{-3}$ Hz.

## 4.2 Measurement results

Several measurements were performed that are discussed below. First, we determined the upper limit of the phase noise induced by the EOM; then, we measured correlations of the EOM's phase shift versus its temperature and the optical power passed through the EOM. Additionally, we examined the phase–temperature correlation of the optical fibre tied to the EOM output.

Figure 5 shows the phase noise calculated from a time series of $\Delta\phi$ as defined in (8) recorded over several hours. The upper limit of the EOM's phase noise (red solid curve) was better than the requirements over the whole frequency range. For comparison, a measurement without amplitude stabilisation is shown (red dashed curve). Here, signal power fluctuations increased the phase noise by about an order of

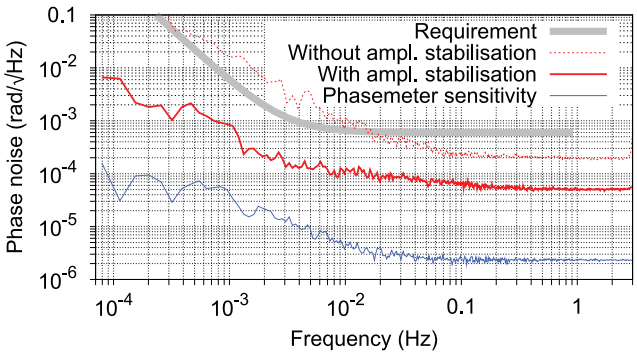


**Fig. 5** Upper Jenoptik EOM spectral phase noise density limit at 2-GHz modulation

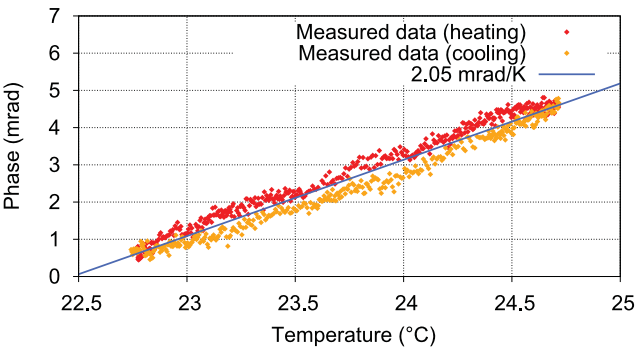


**Fig. 6** Differential phase versus EOM temperature measurement on Jenoptik EOM at 2 GHz

magnitude. The phasemeter sensitivity (blue curve) was well within the required level.

To measure the phase shift caused by a change in the EOM temperature, we constructed a two-part aluminium housing for the EOM with Peltier elements and a heat sink mounted on top. We then intentionally varied the EOM temperature in the range between 22 and 25°C. Multiple temperature sensors were installed in the top and bottom parts. Figure 6 shows a plot of the phase shift induced by the EOM versus its temperature. The measurement data is highlighted in red for the warming periods and in orange for the cool-

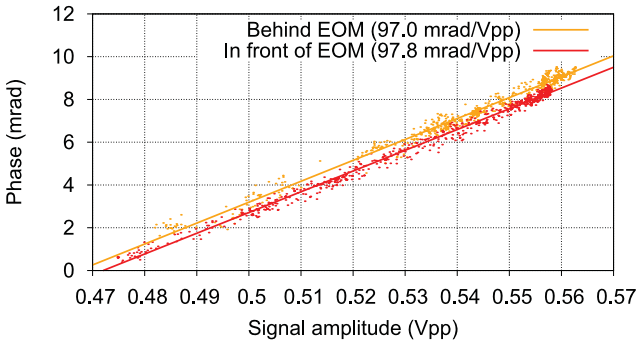


**Fig. 7** Differential phase versus optical power of Laser L1 passed through Jenoptik EOM at 2-GHz modulation

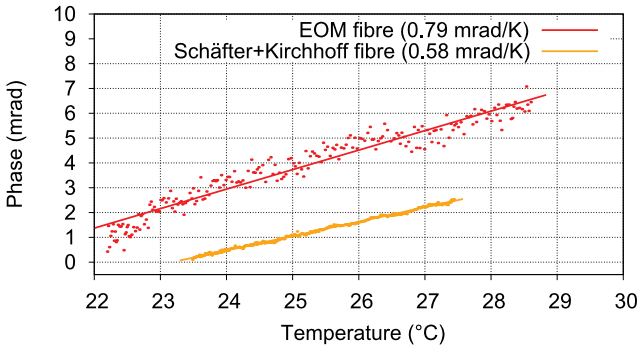


**Fig. 8** Differential phase versus temperature measurement on different optical fibres, scaled to a fibre length of 1 m

ing periods. A linear fit is shown in blue, which presents a dependence of $2.05 \pm 0.03\,\mathrm{mrad/K}$.

The magnitude of the photorefractive effect of the EOM waveguide was determined by altering the laser power going through the EOM by detuning and tuning the EOM's fibre coupling a number of times in short intervals. While doing so, we measured the differential phase $\Delta\phi$ as well as the signal amplitude of the 1.6-kHz sideband–carrier beat note ($U_{\mathrm{LF}} \propto A_{\mathrm{L1}} J_1(m) \times A_{\mathrm{L2}}$). In Fig. 7 the differential phase is plotted against the signal amplitude. Changing the laser power in front of the EOM led to a phase change over signal amplitude correlation of $97.0 \pm 0.4\,\mathrm{mrad/V_{pp}}$ (red curve), while changing the power behind the EOM led to $97.8 \pm 0.3\,\mathrm{mrad/V_{pp}}$ (orange curve). Therefore, the EOM influence was $0.8 \pm 0.7\,\mathrm{mrad/V_{pp}}$ ($0.003 \pm 0.002\,\mathrm{mrad/mW}$). As a result, the EOM's phase dependence on the optical power passed through the EOM was $0.005\,\mathrm{mrad/mW}$ in the worst assumable case. This results in a requirement on the laser power stability on board the LISA spacecraft of $125\,\mathrm{mW}/\sqrt{\mathrm{Hz}}$. The designed power stability of the LISA lasers is orders of magnitude better than this requirement for various other reasons. Therefore, the photorefractive effect of the EOM under test will be negligible.

Since optical fibres are intrinsically connected to the EOM and since their optical path lengths change due to bending and temperature fluctuations, we measured the differential phase dependence of the fibre's temperature. When changing the temperature of the fibre connected to the output of the EOM (as done with a 38-cm section), the sidebands of the modulated laser light were shifted in relation to the carrier. The results are shown in Fig. 8 (red trace). Scaled to a fibre length of 1 m, the temperature-induced phase shift was measured to be $0.79 \pm 0.12\,\mathrm{mrad/K\,m}$. Therefore, including the 1.5-m fibre connected to the EOM's output, the EOM's phase dependence on its temperature was measured to be $3.2 \pm 0.2\,\mathrm{mrad/K}$. The temperature stability at the LISA optical bench is expected to be better than $10^{-4}\,\mathrm{K}/\sqrt{\mathrm{Hz}}$ at room temperature. Thus, the given stability of the EOM fulfills the phase stability requirements with a large margin.

For comparison, a 3-m section of a Schäfter + Kirchhoff single-mode fibre cable was exposed to a temperature change (Fig. 8, orange trace). Scaled to 1 m, the coefficient here is $0.58 \pm 0.04\,\mathrm{mrad/K\,m}$, which is a more stable correlation compared to the EOM's fibre. The differences in the fibres' phase stability might be explained by the fibres' individual jacketing: the thermal phase shift coefficient of a bare fibre is about four times smaller than the coefficient of a fibre with nylon jacketing [17].

## 5 Conclusions

We presented the sideband phase characteristics of a Jenoptik fibre-coupled integrated EOM for a modulation frequency of 2 GHz in the LISA frequency range (1 mHz to 1 Hz). The upper phase noise limit was almost an order of magnitude better than the required $0.6\,\mathrm{mrad}/\sqrt{\mathrm{Hz}}$, which makes the EOM well suitable for use within LISA with respect to its phase characteristics.

The EOM's phase dependence on transmitted optical power was measured and found to be uncritical for LISA. Additionally, the phase dependence of the EOM to temperature was found to be compatible with the expected temperature noise onboard the LISA satellites.

**Acknowledgements** We gratefully acknowledge support by Deutsches Zentrum für Luft- und Raumfahrt (DLR) (reference 50 OQ 0601) and thank the German Research Foundation for funding the Cluster of Excellence QUEST—Centre for Quantum Engineering and Space-Time Research.



## References

1. D.A. Shaddock, Class. Quantum Gravity **25**(11), 114012 (2008)

2. H. Faulks, K. Gehbauer, A. Hammesfahr, K. Honnen, U. Johann, G. Kahl, M. Kersten, L. Morgenroth, M. Riede, H.R. Schulte, M. Bisi, S. Cesare, O. Pierre, X. Sembely, L. Vaillon, J. Rodriguez-Canabal, F. Reudenauer, S. Marcuccio, D. Nicolini, L. Maltecca, M. Peterseim, M. Rodrigues, D. Hayoun, S. Heys, B.J. Kent, I. Butler, D. Robertson, S. Vitale, Study of the laser interferometer space antenna. Final Tech. Rep., European Space Research and Technology Center (2000)
3. LISA Study Team, LISA. Laser interferometer space antenna for the detection and observation of gravitational waves. An international project in the field of fundamental physics in space. Pre-Phase A Rep., Max-Planck-Institut für Quantenoptik, Garching, Germany (1998)
4. W. Folkner, D. Shaddock, M. Tinto, R. Spero, R. Schilling, O. Jennrich, Candidate LISA frequency (modulation) plan. Presentation at 5th Int. LISA Symp., July 2004
5. R.W. Hellings, Phys. Rev. D **64**(2), 022002 (2001)
6. M. Tinto, F.B. Estabrook, J.W. Armstrong, Phys. Rev. D **65**(8), 082003 (2002)
7. L.W. Couch II, *Digital and Analog Communications Systems* (Macmillan, New York, 1990)
8. M. Tröbs, S. Barke, J. Möbius, M. Engelbrecht, D. Kracht, L. d'Arcio, G. Heinzel, K. Danzmann, J. Phys., Conf. Ser. **154**, 012016 (2009)
9. W. Klipstein, P.G. Halverson, R. Peters, R. Cruz, D. Shaddock, Clock noise removal in LISA, in *Laser Interferometer Space Antenna: 6th Int. LISA Symp.*, ed. by S.M. Merkovitz, J.C. Livas. Am. Inst. Phys. Conf. Ser., vol. 873 (2006), pp. 312–318
10. M. Tinto, J.W. Armstrong, F.B. Estabrook, Class. Quantum Gravity **25**(1), 015008 (2008)
11. J.-P. Ruske, Integriert-optische Bauelementekonzepte zur Führung und Beeinflussung von Licht hoher Leistung und Photonenenergie. Habilitation thesis, Friedrich-Schiller-Universität Jena, Germany (2004)
12. S. Steinberg, Experimentelle Untersuchung optischer Phaseninstabilitäten an Streifenwellenleitern und elektrooptischen Phasenmodulatoren in LiNbO3 unter besonderer Berücksichtigung des Protonenaustausches. Ph.D. thesis, Friedrich-Schiller-Universität Jena, Germany (1994)
13. G. Heinzel, Advanced optical techniques for laser-interferometric gravitational-wave detectors. Ph.D. thesis, Max-Planck-Institut für Quantenoptik, Garching (1999)
14. G. Heinzel, V. Wand, A. Garsia, O. Jennrich, C. Braxmaier, D. Robertson, K. Middleton, D. Hoyland, A. Rúdiger, R. Schilling, U. Johann, K. Danzmann, Class. Quantum Gravity **21**(5), S581 (2004)
15. M. Tröbs, G. Heinzel, Measurement **39**(2), 120 (2006)
16. M. Tateda, S. Tanaka, Y. Sugawara, Appl. Opt. **19**, 770 (1980)
17. M. Tröbs, G. Heinzel, Measurement **142**, 170 (2009)